



ELSEVIER

Available online at www.sciencedirect.com

ScienceDirect

journal homepage: www.elsevier.com/locate/hydro

Electrochemical properties of MgO-coated $0.5\text{Li}_2\text{MnO}_3\text{-}0.5\text{LiNi}_{0.5}\text{Mn}_{0.5}\text{O}_2$ composite cathode material for lithium ion battery

Arun Kumar^a, Renny Nazzario^a, Loraine Torres-Castro^b,
A. Pena-Duarte^a, M.S. Tomar^{a,*}

^a Department of Physics, University of Puerto Rico, Mayaguez 00681, Puerto Rico

^b Department of Physics, University of Puerto Rico, Rio Piedras 00931-3343, Puerto Rico

ARTICLE INFO

Article history:

Received 28 September 2014

Received in revised form

30 December 2014

Accepted 19 January 2015

Available online 19 February 2015

Keywords:

Lithium ion battery

Layered composite

MgO-coating

Raman spectroscopy

ABSTRACT

Pristine and MgO-coated $0.5\text{Li}_2\text{MnO}_3\text{-}0.5\text{LiNi}_{0.5}\text{Mn}_{0.5}\text{O}_2$ (LLNMO) composites were synthesized by carbonate based co-precipitation method for cathode material in Li-ion battery. X-ray diffraction confirmed the layered structure of pure material and no major change in crystal structure with MgO-coating. Raman spectroscopy revealed ionic arrangement corresponding to space group of C2/m and R-3m for Li_2MnO_3 and $\text{LiNi}_{0.5}\text{Mn}_{0.5}\text{O}_2$, respectively. Scanning electron microscopy shows the primary particle size to be less than $0.5\ \mu\text{m}$. The observed increase in charge/discharge capacity with number of cycles can be attributed to more activation of Li_2MnO_3 . However, MgO-coated $0.5\text{Li}_2\text{MnO}_3\text{-}0.5\text{LiNi}_{0.5}\text{Mn}_{0.5}\text{O}_2$ composite cathode showed good cyclability and coulombic efficiency, where lower surface layer resistance may contribute to better performance with MgO-coated LLNMO.

Copyright © 2015, Hydrogen Energy Publications, LLC. Published by Elsevier Ltd. All rights reserved.

Introduction

Significant effort has been devoted in the past decade to investigate low cost, high energy, and safe cathode material for high energy density lithium ion battery. The layer components Li_2MnO_3 and $\text{LiMn}_{0.5}\text{Ni}_{0.5}\text{O}_2$ have interesting prospect [1] at nanoscale. Lithium rich layered oxide materials are attractive cathode materials due to their capacities $>200\ \text{mAh/g}$ [1–4], where large capacity was attributed to the activation of Li_2MnO_3 component with Li-excess beyond 4.4 V vs. Li/Li^+ . The advantage of operating at high voltage and the abundance of nontoxic Mn and Ni makes LLNMO as ideal cathode for next generation economically viable and high energy density Li-ion

rechargeable batteries. However, layered composite oxide cathode showed some drawback including (i) moderate cyclability and (ii) larger first cycle irreversible charge capacity. The individual components Li_2MnO_3 and $\text{LiNi}_{0.5}\text{Mn}_{0.5}\text{O}_2$ of the composite have high impedance [5,6], and different mechanisms have been proposed to understand the first cycle charging behavior and the irreversible charge capacity [7–9]. Whether the irreversible capacity observed during the first cycles is associated with solid electrolyte interface (SEI) film formation or decomposition reaction has been addressed recently [10].

In order to enhance the electrochemical properties related to cycleability of such compound, Co was substituted in the

* Corresponding author. Tel.: +1 787 265 3844.

E-mail address: maharajs.tomar@upr.edu (M.S. Tomar).

<http://dx.doi.org/10.1016/j.ijhydene.2015.01.104>

0360-3199/Copyright © 2015, Hydrogen Energy Publications, LLC. Published by Elsevier Ltd. All rights reserved.

second component $\text{LiNi}_{0.5}\text{Mn}_{0.5}\text{O}_2$, but safety and increased cost are of concern. Studies revealed [11] good cyclability with lesser concentration Co, i.e. $\text{Li}[\text{Li}_{0.2}\text{Ni}_{0.17}\text{Co}_{0.07}\text{Mn}_{0.56}]\text{O}_2$ by controlling the upper voltage. The cyclic degradation is believed to be due to the formation of cracks at the surface during cycling, which could make amorphous crystal surface and hence the capacity degradation. The approach to improve electrochemical properties is by coatings, such as AlP_4 , Al_2O_3 , ZrO_2 , Al_2O_3 , CoPO_4 , and treating by ZnO [12,13]. These coatings attributes to surface property by inhibiting the formation of solid electrolyte interface (SEI) layer and thereby improving fast charge transfer reaction because surface treatment with fluorinated salts, such as NH_4PF_6 , NH_4BF_4 and $(\text{NH}_4)_3\text{AlF}_6$ were found to be beneficial for improving electrochemical properties of the active material [14].

Although, the reason for improvement due to coating is not completely understood yet, for restraining the decomposition of the electrolyte an inactive oxide coating is a good way to avoid the direct contact with electrolyte. It enhances stability of the interphase, decrease the reaction between electrode and electrolyte [15], and avoids the dissolution of Mn in electrolyte by collecting HF from electrolyte [16]. Nevertheless, oxide material coating layer may cause loss in capacity and rate capability because of poor electronic and ionic conductivity. In the present work, we used MgO coating on $0.5\text{Li}_2\text{MnO}_3-0.5\text{LiNi}_{0.5}\text{Mn}_{0.5}\text{O}_2$ composite and investigated the structural and electrochemical properties.

Experimental

We synthesized $0.5\text{Li}_2\text{MnO}_3-0.5\text{LiNi}_{0.5}\text{Mn}_{0.5}\text{O}_2$ material by carbonate based co-precipitation method. Nickel (II) sulfate hex-hydrate (Sigma–Aldrich 99%), manganese (II) sulfate monohydrate (Sigma–Aldrich 98%) and lithium carbonate (Strem Chemicals 99.999%) were used as precursors for synthesizing $0.5\text{Li}_2\text{MnO}_3-0.5\text{LiNi}_{0.5}\text{Mn}_{0.5}\text{O}_2$ powders by co-precipitation method. The aqueous solution of 0.2 M of the $\text{MnSO}_4\cdot\text{H}_2\text{O}$ and $\text{NiSO}_4\cdot 6\text{H}_2\text{O}$ was precipitated against 1 M aqueous solution of sodium bicarbonate (NaHCO_3) in a flask with continuous string at 200 rpm at constant temperature of 60°C . The pH of solution was kept at 9 by adding ammonium hydroxide solution (NH_4OH) (Sigma Aldrich 28–30 %). After complete precipitation of Ni and Mn sulfate solution on carbonate solution, the mixture was left for 12 h at 60°C with constant stirring. Then solution were filtered and washed with distilled water. Wet final powder was dried for 12 h at 100°C to get nickel manganese carbonate powder. The obtained powder was mixed with 2% excess amount of lithium carbonate and grounded using a mortar and pestle. Finally, the mixture was calcined at 950°C for 12 h and then quenched at room temperature. MgO (1.5%) solution was added to the suspension of $0.5\text{Li}_2\text{MnO}_3-0.5\text{LiNi}_{0.5}\text{Mn}_{0.5}\text{O}_2$ (98.5%) and stirred for 1 h for to achieve MgO-coated $0.5\text{Li}_2\text{MnO}_3-0.5\text{LiNi}_{0.5}\text{Mn}_{0.5}\text{O}_2$ powder. Finally, NH_4OH solution was added to suspension and pH was adjusted to 11 in order to get effective precipitation of MgO. The powder sample obtained was dried overnight at 110°C in air and calcined at 500°C for 1 h.

X-ray diffraction (XRD) with Cu K_α radiation (Siemens D5000) was used for collecting the patterns in the range 15° to 80° (2θ scale) with 0.02 step size and 5 s counting time. Scanning electron microscopy (SEM) analysis was conducted with JEOL 7600 FESEM system interfaced to a Thermo-Electron System Microanalysis Systems. Raman-scattering data were obtained using a T64000 spectrometer equipped with a triple-grating monochromator and a Coherent Innova 90C Ar⁺-laser at 514.5 nm.

The electrochemical properties of the synthesized powder were carried out in two electrode CR2032 type coin cell configuration using liquid electrolyte consisting of LiPF_6 (1M) dissolved in 1:1 (by weight) mixture of ethylene carbonate (EC) and dimethyl carbonate (DMC). The working electrode was prepared by mixing calcined powder, polyvinylidene fluoride, and carbon black in 80:10:10 weight ratio. A slurry was prepared using N-methyl pyrrolidone (NMP) as solvent and the slurry was spread on Al foil and kept for drying under vacuum at about 110°C for 6 h. Li metal foil was used as anode and celgard 2400 was used as separator between anode and cathode. The coin cell was assembled in Ar atmosphere inside a glove box (MBraun). The electrochemical measurements were performed on a computer controlled potentiostat/galvanostat system (consisting a PC 750.4 controller and PHE 200 software [Gamry Instrument]). The charge discharge measurements were performed at room temperature in the voltage range 2.0–4.8 V using selected current density.

Result and discussion

Pristine and MgO-coated $0.5\text{Li}_2\text{MnO}_3-0.5\text{LiNi}_{0.5}\text{Mn}_{0.5}\text{O}_2$ composite material was studied for structural and impedance properties, and electrochemical (cyclability and coulombic efficiency) characterization.

Structure and Morphology

XRD patterns of the synthesized pristine and MgO-coated $0.5\text{Li}_2\text{MnO}_3-0.5\text{LiNi}_{0.5}\text{Mn}_{0.5}\text{O}_2$ (LLNMO) powder is shown in Fig. 1. It shows the typical diffraction pattern of LLNMO layered material, where every peak (except those which are between $2\theta = 20-30^\circ$) agree well with the R3m (JCPDS #09-0063) space group of the $\alpha\text{-NaFeO}_2$ structure. The low intensity peaks between 20 and 30° show monoclinic Li_2MnO_3 phase with space group C2/m (JCPDS# 84-1634). A clear distinction of the peak (006) and (012) show the formation of well crystalline layered structure without spinal structure [1]. At the nanoscopic level two different kind of crystal structures are possible because of the close-packed layer which have an interlayer spacing close to 4.6 Å [4]. The observed two phases corresponds to the lower symmetry C2/m and higher symmetry R3m space groups, suggesting the successful formation of composite structure. XRD pattern of MgO-coated LLNMO powder is identical to that of the pristine LLNMO powder, indicating the absence of reflections corresponding to MgO lattice plane due to lower concentration.

Raman spectra corresponding to the pristine LLNMO and MgO-coated LLNMO are shown in Fig. 2(a, b). In earlier work, Raman studies on LLNMO have shown [17] three major Raman

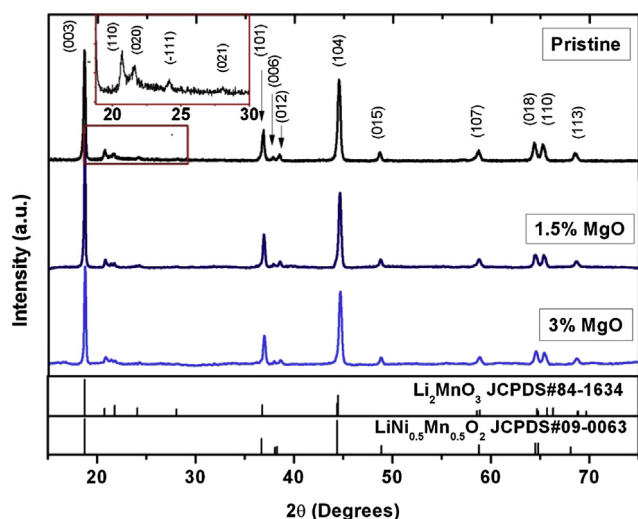


Fig. 1 – XRD patterns of the composite cathodes of $0.5\text{Li}_2\text{MnO}_3\text{-}0.5\text{LiNi}_{0.5}\text{Mn}_{0.5}\text{O}_2$.

active modes at 424, 476 and 594 cm^{-1} with some indistinctive bands between 200 and 400 cm^{-1} . Although, layered lithium metal oxide with rhombohedral R_{3m} symmetry showed $A_{1g} + E_g$ Raman active mode [18], theoretical calculation based on $C_{2/m}$ symmetry indicates six Raman active mode $2A_g + B_g$ [19], and also the presence of Li_2MnO_3 in LLNMO composite structure in lower frequency at 424 cm^{-1} . In the present work, three major Raman active mode have been identified in Fig. 2(a, b) at 424, 476 and 594 cm^{-1} for both pristine LLNMO and MgO-coated LLNMO, which is in agreement with earlier researchers on the composite cathode composed of Li_2MnO_3 and $\text{LiNi}_{0.5}\text{Mn}_{0.5}\text{O}_2$ [17]. No change in the Raman active mode positions was observed in MgO-coated LLNMO.

Morphology of the material was examined using scanning electron microscopy (SEM) and is shown in Fig. 3(a, b). Primary particles are in micron size and spherical agglomerates. The agglomerates of relatively smaller primary particles are considered favorable for better charge/discharge capacity due

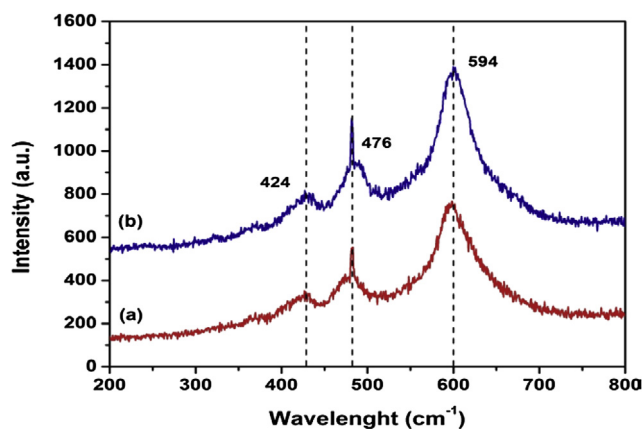


Fig. 2 – Raman spectra of (a) Pristine LLNMO, and (b) MgO-coated LLNMO in $250\text{--}800\text{ cm}^{-1}$ range.

to their higher trap density [20] that shortens the lithium diffusion. Pristine LLNMO composite have highly agglomerates compared to MgO-coated LLNMO, which helps to increase specific capacity. Primary particle size in the case of LLNMO and MgO-coated sample were between 0.5 and $1\text{ }\mu\text{m}$.

Electrochemical properties

Charge/discharge profile of the pristine and MgO-coated LLNMO are shown in Fig. 4(a, b). First charge/discharge profile observed to be sloppy in both pristine LLNMO and MgO-coated LLNMO composite cathode. Earlier reports explained this type of behavior [21] when Co is replaced with Ni and Mn which changes the phase transformation process and finally resulting sloppy nature in charge/discharge curve [2,22]. Higher discharge capacity has been observed in the case of pristine LLNMO compared to MgO-coated LLNMO. The discharge capacity in the first cycle is approximately identical in 3–3.5 V Fig. 4 shows the charge–discharge capacity at room temperature for 1st, 2nd, 5th 10th and 20th cycles with LLNMO and also for MgO-coated LLNMO composite electrode at 15 mA/g current density between 2 and 4.8 V for 19th and 25th cycles. Continuous activation of Li_2MnO_3 over the voltage range 2–4.8 V and the final highest discharge capacity occurs at about 19 cycles for pristine. For MgO-coated LLNMO layer composite highest discharge capacity occurs after 15 cycles. The activation of Li intercalation/deintercalation between 3.5 and 3 V considerably contributes to increase the overall capacity. Thus, for pristine LLNMO the capacity gradually increases from 130 mAh/g in first cycle to 223 mAh/g for 20 cycles. After full activation of Li_2MnO_3 component in the present structure, the discharge capacity is 230 mAh/g and 73% columbic efficiency. With MgO-coated LLNMO cathode, the first discharges capacity is 124 mAh/g and after 25th cycle the discharge capacity is 143 mAh/g with 75% columbic efficiency as shown in Fig. 4 (b). MgO-coated composite have low discharge capacity because the oxide coating may have low electronic and ionic conductivity. Morphology shows that the particle are uniformly distributed, so that lithium have low migration in comparison to the pristine LLNMO composite cathode.

Fig. 5 shows the cyclability for the 50 cycle at constant 15 mA/g current density, where this experiment sample was kept at fully charge state at 4.8 V for about 20 min before discharge to ensure the structure stability. In pristine charge/discharge capacity continues increase up to 19th cycle and then fall down while the charge/discharge capacity has been observed quite stable up to 50 cycle in MgO-coated LLNMO. These results clearly indicate that MgO coating improve the columbic efficiency from 73 % to 75 %, which means less irreversible capacity and less than 7% of capacity fade after 50 cycle discharge which is a good capacity retention. This stable behavior in electrochemical performance makes MgO-coated LLNMO a good candidate for low cost and nontoxic cathode material for lithium ion battery.

Impedance of the electrochemical cell is a crucial parameter to determine its performance. Electrochemical impedance spectroscopy (EIS) is used to determine electrochemical cell impedance in response to small ac signal at constant DC voltage over wide frequency range from MHz to mHz [23]. EIS

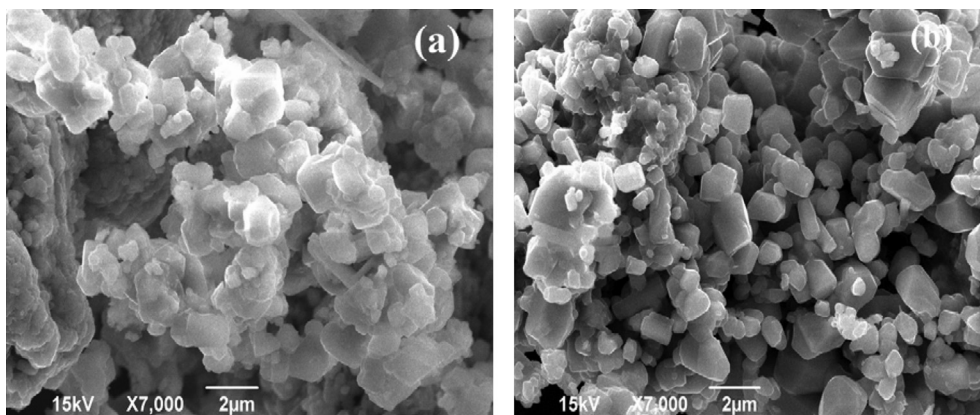


Fig. 3 – Scanning electron microscopy (SEM) (a) pristine LLNMO showing the agglomerates of primary particles, and (b) MgO-coated LLNMO composite cathode.

measurement have been carried out on the coin cell and the results are shown in Fig. 6 (a) - 1st cycle, and Fig. 6 (b) - 20th cycle in Nyquist plot. Various models have been proposed in the past to explain the EIS data [24].

The model used for fitting the current data is shown in Fig. 7. The appearance of two suppressed semicircles suggests the contribution of two different resistance elements – R_{sf} due to surface layer by solid electrolyte formation [25] at high

frequency and the charge transfer resistance R_{ct} across the interface. Capacity fading of cathode material is due to SEI layer which grows thicker by electrolyte–electrode reaction during charge/discharge and deteriorates the performance. Analysis of the data indicates that the major contribution to the impedance is from R_{sf} and R_{ct} because the observed intrinsic capacitance C_{int} is almost same in both cases. The diffusion coefficient Z_w is highest ($16.43e^{-7} \text{ cm}^2\text{S}^{-1}$) in pristine LLNMO which facilitates diffusion of lithium in solid material. Increase in R_{sf} in both cases is expected because of the growth of SEI layer at the interface of the electrolyte and electrode surface. In pristine LLNMO composite it increases rapidly, and additional resistance is added to increase R_{sf} in MgO-coated LLNMO. After 20 cycles, R_{sf} is low in MgO-coated sample in comparison with pristine LLNMO. Thus, MgO-coated LLNMO composite layer should have more structure stability and improved cyclability during charge/discharge reaction.

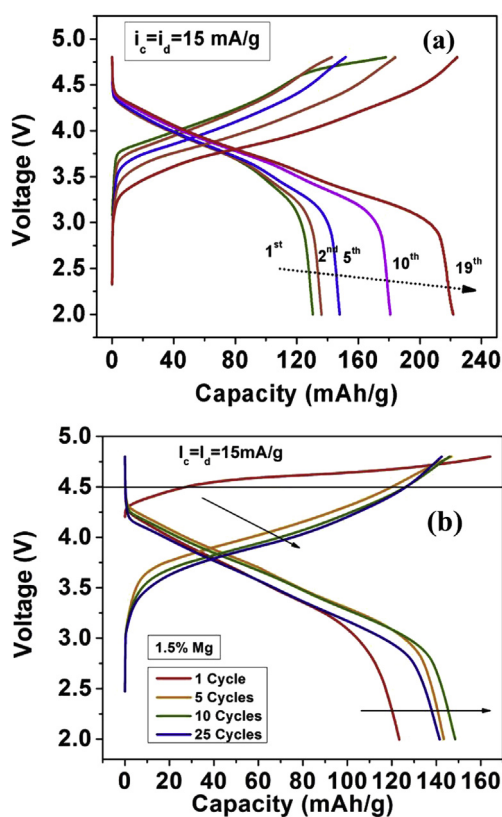


Fig. 4 – Charge/discharge curve for different cycles at 15 mA/g (a) pristine LLNMO (b) MgO-coated LLNMO.

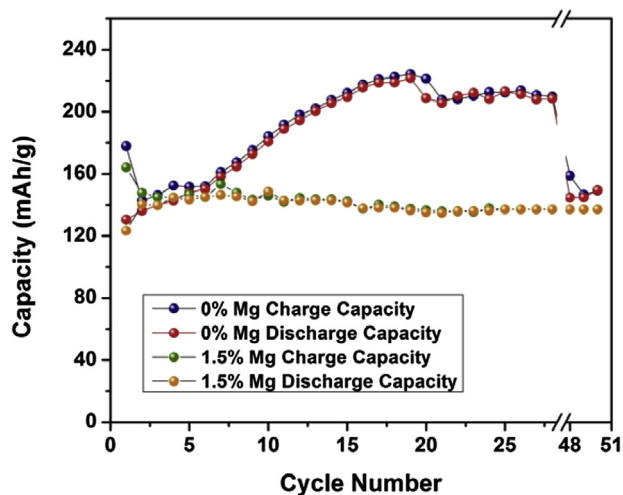


Fig. 5 – Charge/discharge capacity vs. cycle number at constant current density for pristine and MgO-coated LLNMO.

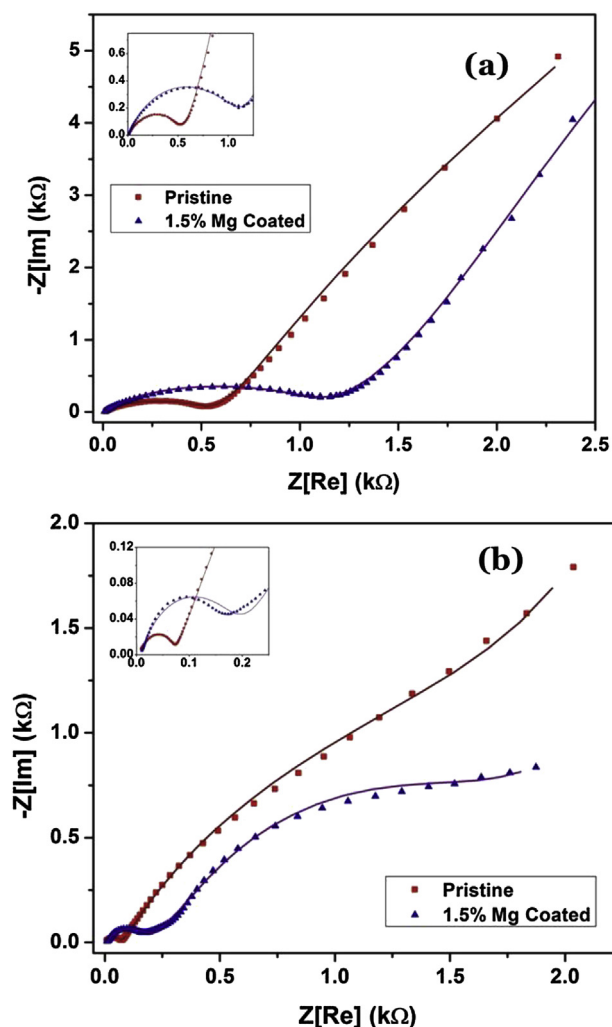


Fig. 6 – Nyquist plots obtained from EIS spectroscopy of pristine and MgO-coated LLNMO (a) after 1st cycle (b) after 20th cycle.

Conclusion

In order to improve the electrochemical properties (cyclability) of Li-ion battery, pristine and MgO coated $0.5\text{Li}_2\text{MnO}_3-0.5\text{LiNi}_{0.5}\text{Mn}_{0.5}\text{O}_2$ cathode materials were used. Materials were synthesized by co-precipitation method. Results

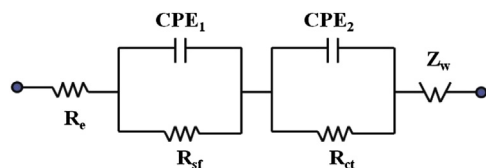


Fig. 7 – Fitted model for EIS spectra, where R_e —electrolyte resistance, R_{sf} —surface layer resistance, R_{ct} —charge transfer resistance, CPE—constant phase element and Z_w —Warburg impedance.

indicates that MgO-coated LLNMO restrains the subsidiary reaction between electrode and electrolyte during charge/discharge reaction. It also stabilizes the structure of the composite as indicated by improve columbic efficiency from 73 % to 75 % - meaning less irreversible capacity. After 50 cycles at 15 mA/g which indicates good capacity retention. Further work is required to optimize MgO content to get best specific capacity.

Acknowledgments

One of us (MST) appreciates the help of Dean of Research and the office of Vice Chancellor, University of Puerto Rico, Mayaguez, PR.

REFERENCES

- [1] Lu Zhonghua, Beaulieu LY, Donaberger RA, Thomas CL, Dahan JR. *J Electrochem Soc* 2002;149:A778.
- [2] Lu Zhonghua, Dahn JR. *J Electrochem Soc* 2002;149:A815.
- [3] Barkhouse DAR, R Dahn J. *J Electrochem Soc* 2005;152:A746.
- [4] M Thackery M, Kang S-H, Johnson CS, Vaughey JT, Benedek R, Hackey SA. *J Mater Chem* 2007;17:3112.
- [5] Huiming Wu, Ilias Belharouak, Yang-Kook Sun, and Khalil Amine. Abstract #290, 218th ECS Meeting.
- [6] Xiu Qin Song, Jian-Feng Ma, Ru-Fen Chen. *J Inorg Mater* 2001;15:37.
- [7] Van Bommel Andrew, Krause LJ, Dhan JR. *J Electrochem Soc* 2001;158:A731.
- [8] Jiang Meng, Key Baris, Meng Ying S, Grey Clare P. *Chem Mater* 2003;21:2733.
- [9] Robertson Alastair D, Bruce Peter G. *Chem Commun* 2002:2790.
- [10] West WC, Staniewicz RJ, Ma C, Robak J, Soler J, M. C., et al. *J Power Source* 2004;196:9696.
- [11] Ito Atsushi, Li Decheng, Ohsawa Yasuhiko, Yuichi Sato J. *Power Source* 2008;183:344.
- [12] Wu Y, Manthiram A. *Solid State Ion* 2009;180:50.
- [13] Singh Gurpreet, Thomas R, Kumar Arun, Katiyar RS, Manivannan A. *J Electrochem Soc* 2002;159:A470.
- [14] Kang SH, Thackerey MM. *J Electrochem Soc* 2008;155:A269.
- [15] Shaju KM, Subha Rao GV, Chowdari BVR. *Electrochim Acta* 2002;48:145.
- [16] Han Enshan, Liu Xiangtao, Zhu Lingzhi, Pan Chao, Wu Zhiqin. *Ionics* 2013;19:997–1003.
- [17] Hong Jihyun, Dong-Hwa Seo, Sung-Wook Kim, Gwon Hyeokjo, Song-Taek Oh, Kang Kisuk. *J Mater Chem* 2010;20:10179.
- [18] Zhang Lianqi, Takada Kazunori, Ohta Narumi, Fukuda Katsutoshi, Osada Minoru, Wang Lianzhou, et al. *J Electrochem Soc* 2005;152:A171.
- [19] Inaba M, Iriyama Y, Ogumi Z, Todzuka Y, Tasaka A. *J Raman Spectrosc* 1997;28:613.
- [20] Deng Haixia, Belharouak Ilias, Kook Sun Yan-, Khalil Amine J. *Mater Chem* 2009;19:4510.
- [21] Ma Jianxin, Wang Chunsheng, Shannon Wroblewski J. *Power Source* 2007;164:849.
- [22] Robertson AD, Bruce PG. *Chem Mater* 1984;2003:15.
- [23] Ratnakumar BV, Smart MC, Surampudi S. *Chem Inf* 2002;33:229.
- [24] Levi MD, Aurbach D. *J Electrochem Soc* 1999;146:1279.
- [25] Ning G, Haran B, Branko N. *J Power Source* 2003;117:160.